Biochimica et Biophysica Acta 938 (1988) 279–292
Elsevier

BBA 73876

Two untilted lamellar packings for an ether-linked phosphatidyl-*N*-methylethanolamine. An electron crystallographic study

Douglas L. Dorset

Electron Diffraction Department, Medical Foundation of Buffalo, Inc., Buffalo, NY (U.S.A.)

(Received 13 July 1987)

Key words: Phospholipid; Crystal structure analysis; Epitaxial crystallization; Electron diffraction; Electron microscopy; Densitometry

Electron diffraction intensity data from epitaxially crystallized samples of 1,2-dihexadecyl-*sn*-glycero-3-phospho-*N*-methylethanolamine are used to determine the lamellar packings of two polymorphic forms. One form is a typical bilayer structure, with untilted acyl chains packing in the hexagonal methylene subcell and resembles the structures of dihexadecylphosphatidylethanolamine (DHPE) and -choline (DHPC). The lamellar spacing is very close to that of DHPC, indicating that the initial methylation in itself causes a dramatic change in the bilayer thickness. The second polymorph is an interdigitated structure, again with untilted chains which pack in the orthorhombic perpendicular subcell. Direct electron microscope lattice images have been obtained from both crystal forms at low beam doses to justify the correction of observed electron diffraction intensities for curvilinear lamellar distortions. The use of such image data for phasing low angle diffraction data is also successful.

Introduction

Recently, when the phase behavior of fully hydrated phosphatidylethanolamine derivatives with increasing methylation of the primary amine was studied by X-ray diffraction and differential scanning calorimetry, it was shown that an abrupt change in lamellar spacing occurs after the first amine substitution [1]. Although the increased bulk of the polar group was acknowledged to have some influence on this behavior, the data were thought to suggest instead that increased hydration of *N*-methylated derivatives, in comparison to the poorly hydrated phosphatidylethanolamine, was the major contribution to the greater lamellar thickness.

Correspondence: D.L. Dorset, Electron Diffraction Department, Medical Foundation of Buffalo, Inc., 73 High Street, Buffalo, NY 14203, U.S.A.

Review of the existing X-ray crystal structures for diacylphospholipids does not allow one to interpret these data easily, for although the phosphatidylethanolamine [2,3] and phosphatidylcholine [4] structures reveal the packing requirements for different headgroup sizes [5], as well as the favored hydration of the latter compound, the only existing crystal structure of an intermediate material, i.e. the phosphatidyl-*N*,*N*-dimethylethanolamine [6], involves an interdigitated headgroup packing which is quite distinct from either of the other two structures. X-ray [7,9] and neutron [10–12] diffraction analyses, moreover, indicate that both the phosphatidylethanolamines and phosphatidylcholines have similar headgroup conformations in oriented multilayers where the short ethanolamine chain is more or less parallel to the bilayer surface. Although no quantitative structure analysis has been reported for either the *N*,*N*-dimethyl or *N*-monomethyl derivatives pack-

ing in hydrated multilayers, the rather large lamellar spacings in the hydrated forms [1] may possibly indicate that the interdigitated headgroup packing found in the anhydrous crystal structure is not present since the crystal structure of the dimethyl compound [6] has a smaller bilayer thickness (d_{001} = 39.4 Å) than found for the corresponding unmethylated compound (d_{001} = 47.8 Å) [7]. On the other hand, as pointed out in recent DSC and spectroscopic studies [13], molecular tilt could also be an important factor in determining the thickness of lamellar layers, in addition to the contribution from the hydration layer mentioned above. Thus the prediction of bilayer thickness is complicated by several variables.

This paper is an attempt to determine the importance of headgroup size and/or conformation on the lamellar thickness of *N*-methylated phosphatidylethanolamines. For this purpose electron diffraction experiments are carried out on a sequential series of *N*-methyl derivatives, using the high vacuum of the electron microscope to ensure a minimal hydration of the specimens. Finally, a structure analysis is reported for the monomethyl derivative for which, to our knowledge, no quantitative diffraction investigations have been described.

Materials and Methods

Sample crystallization

N-Methylated or unsubstituted chiral phosphatidylethanol amines in both the ether-linked dihexadecyl series or ester-linked dipalmitoyl series were purchased from Calbiochem-Behring (La Jolla, CA) and used without further purification. (At the time of purchase, the ether-linked *N,N*-dimethyl derivative was not available). All compounds in the series were epitaxially crystallized on naphthalene for a comparison of electron diffraction lamellar spacings. This crystallization, which exploits the lattice match between the major naphthalene crystal face and the lateral packing distance between polymethylene chains [14] has been used successfully to orient a variety of lipids [15] so that that longest unit cell axis is parallel to the major crystal face rather than normal to it. (The latter orientation is present in the usual crystal growth from solution [16].) Either of two methods are used for epitaxial crystallization. One, described by Fryer [17], requires a small amount of the lipid to be added to an excess of naphthalene. When the physical mixture is melted to form a dilute solution, a carbon film-covered electron microscope grid is dipped into the molten mass, withdrawn, and allowed to cool. Alternatively, using the method of Wittmann and Manley [14], a dilute solution of the lipid is first evaporated onto a freshly cleaved mica sheet. Carbon covered grids are then placed over areas containing the thin lipid film after which naphthalene is sprinkled around the grids. The other mica sheet is placed over this array to form a sandwich which is then moved along a thermal gradient to melt the naphthalene which solubilizes the lipid. Upon cooling, epitaxial growth takes place, e.g. on the grid surface. The naphthalene can be removed from the grid surface in either case by sublimation in vacuo, leaving the oriented microcrystals on the carbon film.

In order to determine acyl chain packing, dilute solutions of 1,2-dihexadecyl-*sn*-glycero-3-phospho-*N*-methylethanolamine (DHPEM) were made up in either warm chloroform or warm ethanol. These solutions were then evaporated onto a carbon film covered grid surface to produce the more typical crystal form with molecular axes more or less perpendicular to the best developed lamellar face.

Electron diffraction

Selected area electron diffraction patterns obtained at 100 kV on a JEOL JEM-100B electron microscope were photographed under usual low beam dose conditions [18] on either Kodak NS5T or DEF-5 X-ray films. Camera lengths for the diffraction experiments were calibrated with a polycrystalline gold standard from which Debye-Scherrer patterns are photographed at electron microscope lens settings identical to those used to obtain the lipid diffraction patterns. Generally two camera lengths were selected for each microcrystalline sample, a smaller one to visualize the lamellar resolution of the diffraction pattern and a larger one to separate the lowest angle reflection from the background intensity around the central beam.

Electron microscopy

Low-dose electron micrographs of the lamellar repeat in epitaxially crystallized lipid samples were photographed on Kodak DEF-5 film, employing the methodology described recently by Fryer and Dorset [19]. In general, the electron microscope is first adjusted for objective lens astigmatism at a magnification much higher than the one used to photograph the image (e.g. 100 000 ×). The illumination is adjusted to the low beam currents used for electron diffraction and a direct magnification of around 20 000 × is used for the experiment. The grid is then searched for suitable specimens in the diffraction mode. When a suitably good sample is found, the image mode is selected and the grid translated to a nearby area which is brought into focus. Returning to the original area, a sequence of three micrographs is photographed at successive under-focus steps, after which the survival of the specimen in the electron beam is confirmed by electron diffraction. For 'dead time' between exposures or during the selection of alternate microscope functions, the beam can be swept away from the specimen area by use of deliberately misaligned 'dark field' controls of the beam deflector coils near the condensor lenses.

Densitometry

Electron diffraction intensities are obtained from slit aperture scans or diffraction films with a Joyce Loebl MkIIIC flat bed microdensitometer, using a triangular approximation of the densitometer peak area. It is often seen in our work with those phospholipids that the arcing of high order lamellar reflections is similar to the diffraction from epitaxially oriented phosphatidylethanolamine microcrystals [20], for which low dose electron microscope 'lattice images' depict the presence of paracrystalline curvilinear distortion of the bilayer lamellae [19,20]. An appropriate correction [20] is made for this crystal texture to obtain observed structure factor magnitudes, i.e.

$$|F_{00l}^{obs}| = k(I_{00l}^{obs} l)^{1/2}$$

where l is the order of the lamellar reflection, and k is a scale factor.

Low dose lattice images of the lamellar packing were initially evaluated on an optical bench to detect crystalline regions (which may or may not be visible to the eye). These areas were then scanned on an Optronics P1000 rotating drum microdensitometer with a 25 μm raster width to create an image pixel density file on a VAX 8600 computer.

Crystal structure analysis

Structure analysis is based on the combined use of one-dimensional Patterson functions and structural models based on conformers of 1,2-dimyristoyl-*sn*-glycero-3-phosphocholine [4] (see Fig. 3). Patterson functions are calculated in the usual way, i.e.

$$P(w) = \Sigma |F_{00l}|^2 \cos 2\pi lz$$

where z is a fractional coordinate along c and w is its corresponding distance in Å. Models are compared to observed structure factor magnitude by calculation of kinematical structure factors

$$F_{00l} = \sum_j f_j' \exp 2\pi i(\vec{r}_j \cdot \vec{s}_{00l})$$

$$= 2\sum_j f_j' \cos 2\pi(\vec{r}_j \cdot \vec{s}_{00l})$$

which have centrosymmetric phases due to a 2-fold dyad axis parallel to the crystallographic b-axis in all the phospholipid crystal structures reported so far. Here f_j' is a Doyle-Turner electron scattering factor [22] corrected for isotropic thermal motion. Following Hitchcock et al. [7], the isotropic temperature factor B_j for atom j is approximated by $B_j = (C + 4.0 + 108z_j^2)$Å^2 where $C \cong 0.0$ Å^2 for molecular crystals [21]. The structure analysis progresses with a suitable molecular conformation suggested from known phospholipid structures which is translated past the unit cell origin to seek a minimum in the crystallographic residual

$$R = \frac{\Sigma||F_{00l}^{obs}| - k|F_{00l}^{calc}||}{\Sigma|F_{00l}^{obs}|}$$

Since the numbers of observed data and refineable parameters are not very different, this identification of a correct structure cannot be very precise [23]. For this reason, a match of Patterson functions generated from observed and calculated data

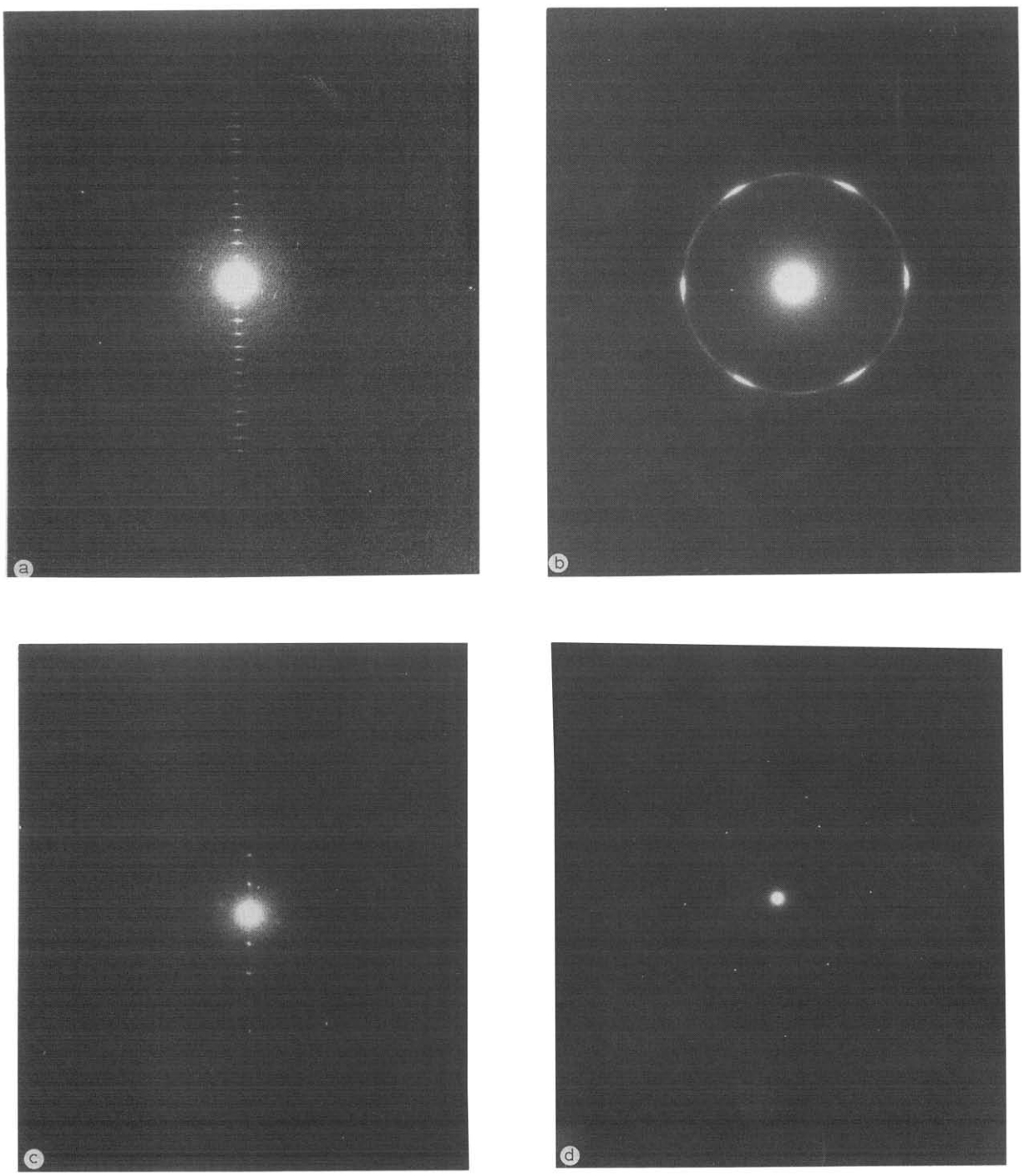

Fig. 1. (a) Lamellar electron diffraction pattern from DHPEM, form 1, epitaxially crystallized onto naphthalene (the so called 'meridional' reflections, which are perpendicular to other depicted lamellar reflections and represent the methylene chain side-to-side packing, are not shown), $d_{001} = 58.4 \pm 0.3$ Å. (b) Electron diffraction patterns from solution crystallized DHPEM, form 1, characteristic of the heagonal methylene subcell $d_{100} = 4.10 \pm 0.06$ Å. (c) Lamellar electron diffraction pattern from DHPEM, form 2, epitaxially crystallized onto naphthalene (meridional reflection not shown), $d_{001} = 33.4 \pm 0.5$ Å. (d) Electron diffraction pattern from solution-crystallized DHPEM, form 2, characteristic of the orthorhombic perpendicular subcell, $d_{100} = 7.69$ Å, $d_{010} = 5.08$ Å. As stated in another paper [20], the lamellar intensities are corrected for crystal distortions in a way consistent with earlier X-ray analyses of oriented phospholipid multilayers (e.g. compare the raw intensity data for DMPE [43] to those used for structure analysis [7]).

is used as another criterion [21] for the correctness of a structural model.

Image analysis

The image file created by an Optronics densitometer scan can be manipulated with image processing software such as IMAGIC [24]. In our work, so-called Fourier-peak-filtered images were created from the experimental images. This is done by overlaying a mask onto the computed image Fourier transform which would pass only the peak amplitudes and phases within a certain hole radius for each Bragg diffraction spot when this simulated optical diffraction pattern forms a presumably noise-free image of the lamellar repeat in the reverse Fourier-transform. It is assumed that the continuous diffraction in the calculated optical transform is due only to noise and should be filtered out.

Phases and amplitudes are also obtained during the calculation of the image transform and stored as a separate file. The phases are directly related to the crystallographic phases of the phospholipid structure within the small phase error due to the information transfer properties of the electron microscope objective lens [25]. These phases can be retrieved by determination of the appropriate unit cell translation, r_0, to reach a crystallographic phase origin [26]. That is, if the electrostatic potential $\rho(r)$ is origin-shifted, i.e.:

$$g(r) = \rho(r) * \delta(r + r_0) = \rho(r + r_0)$$

(where $*$ denotes convolution), then the Fourier transform of $g(r)$, $G(l) = F(l)\ \exp 2\pi i s \cdot r_0 = |F(l)|\ \exp i(\alpha + 2\pi s \cdot r_0)$ contains an additional phase term which expresses this origin shift [27].

Results

Electron diffraction measurements

For *N*-methylated C_{16} acyl chain phosphatidylethanolamines, it is readily apparent that the lamellar spacing increase takes place after a single *N*-methylation in minimally hydrated structures just as it does for fully hydrated crystal forms [1] (i.e. the d_{001} spacings measured from electron diffraction patterns are: DPPE, 55.0 ± 0.3 Å; DPPEM, 57.4 ± 0.5 Å, $DPPEM_2$, 58.7 ± 0.4 Å, DPPC, 57.9 ± 0.9 Å). The ether-linked compounds may have slightly longer lamellar spacings than the ester-linked lipids (i.e. electron diffraction values are: DHPE, 55.6 ± 0.5 Å; DHPEM, 58.4 ± 0.3 Å; DHPC, 59.2 ± 0.5 Å). The increase in lamellar spacing, therefore, appears to be almost step-like within this observational error rather than a gradual rise, an observation consistent with measurement of lower temperature forms of fully hydrated material [1].

When the diether phosphatidyl-*N*-methylethanolamine DHPEM was originally crystallized on a naphthalene substrate, a diffraction pattern from the bilayer structure was observed as shown in Fig. 1a. Observed $0k0$ meridional reflections at $(4.19\ \text{Å})^{-1}$ in these lamellar diffraction patterns

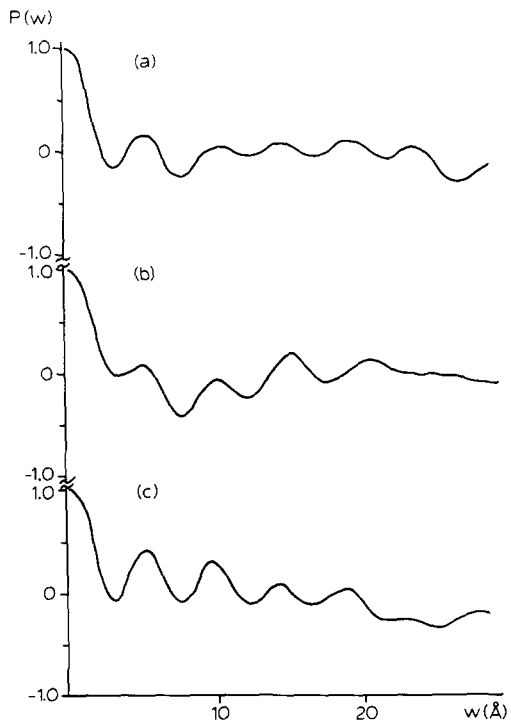

Fig. 2. Patterson functions for DHPEM, form 1: (a) observed electron diffraction intensities corrected for curvilinear lamellar distortions, major peaks at 5.3 Å, 9.9 Å, 14.3 Å, 19.0 Å; (b) calculated data for model with *N*-methylethanolamine chain perpendicular to bilayer surface (Fig. 3) at *R*-factor minimum (Fig. 6), major peaks at 4.7 Å, 9.9 Å, 15.2 Å, 20.4 Å; (c) calculated data for model with *N*-methylethanolamine chain parallel to bilayer surface (Fig. 3) at *R*-factor minimum (Fig. 6), major peaks at 5.0 Å, 9.3 Å, 14.0 Å, 18.7 Å.

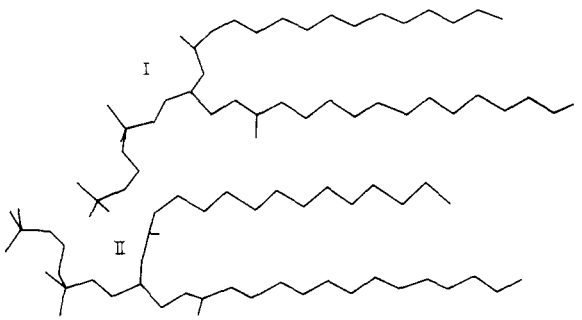

Fig. 3. Two headgroup conformations found in the X-ray crystal structure analysis of DMPC by Pearson and Pascher [4]. Models for form 1 of DHPEM are based on the atomic coordinates, individually considering each possible *N*-methyl atom position in separate translational structure analyses.

correspond to the $d_{100} = 4.10 \pm 0.06$ Å spacing of the hexagonal methylene subcell [28] seen in electron diffraction patterns from solution crystallized specimens (Fig. 1b). It is apparent that the chain axes are normal to the bilayer surface in this polymorph, which is designated form 1.

A subsequent epitaxial crystallization was found to yield another polymorph, here termed form 2, with a much smaller lamellar spacing (Fig. 1c). Meridional reflections in the lamellar diffraction patterns occur at $(2.46 \pm 0.01$ Å$)^{-1}$ corresponding to the 020 spacing of the orthorhombic perpendicular subcell [28]. Again electron diffraction patterns from solution crystallized phospholipid can be used to distinguish the features of the hydrocarbon chain packing [29]. A corresponding diffraction pattern from this crystal form which is grown from organic solvent is shown in Fig. 1d. This *hk*0 electron diffraction pattern is characteristic of untilted chain packing in the $O_\perp$ methylene subcell as shown earlier [29] and is found for numerous materials, including *n*-paraffins.

By chance, the two epitaxial crystallizations initially produced uniform samples of one crystal form or the other, but subsequent preparations indicated that the two forms could be simultaneously produced on the same grid surface. This finding for epitaxially crystallized samples is similar to the occurrence of various polymorphic forms of a phospholipid when crystallized from evaporated solution onto a grid surface [30].

Crystal structure analysis

Form 1

A one-dimensional Patterson function calculated from observed electron diffraction intensities corrected for paracyrstalline lattice distortions is depicted in Fig. 2a for the form 1 structure with longest lamellar repeat. Major autocorrelation peaks are found at 5.3 Å, 9.9 Å, 14.3 Å and 19.0 Å, reminiscent of structure analyses for sphingomyelin using X-ray diffraction data [31] as well as a series of phosphatidylethanolamines [20] and an ether-linked phosphatidylcholine [32] based on electron diffraction data. As argued in the X-ray analysis of sphingomyelin [31], but also found in the X-ray crystal structures of diacylphospholipids cited above, conformational features of the non-headgroup moiety are often conserved in these structures, particularly in terms of a one-dimensional structure analysis.

Two headgroup conformations are found in the crystal structure of DMPC [4], as shown in Fig. 3. In our recent structure analysis of the ether-linked analog DHPC [32], only one conformation with the choline group parallel to the bilayer surface

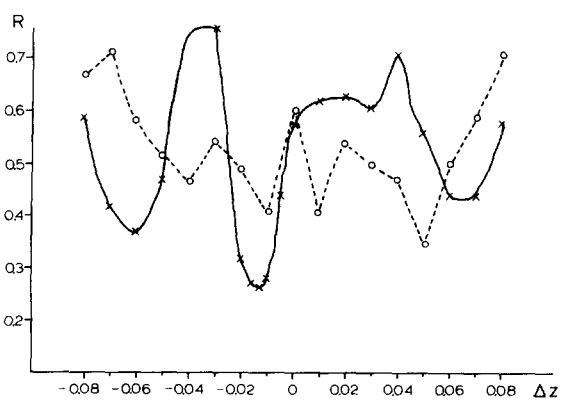

Fig. 4. Re-analysis of the crystal structure of DHPC based on a corrected *N*-methyl coordinate but also considering both headgroup conformers in Fig. 3. The molecule is shifted Δz by the unit cell origin. For the form with choline parallel to the bilayer surface (solid line); the distinction between the two lowest *R*-factor minima seen earlier [28] is more clear, corresponding to the crystal structure identified by matching of Patterson functions. The Patterson function calculated for the perpendicular headgroup conformation (dashed line *R*-factor plot) has no resemblance to the observed autocorrelation function (Fig. 5).

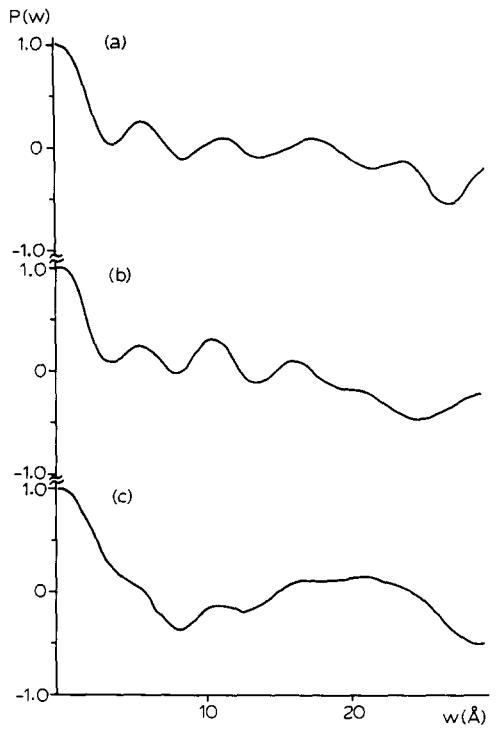

Fig. 5. Patterson functions for DHPC: (a) observed electron diffraction data, (b) calculated data for choline conformation parallel to bilayer surface at lowest *R*-factor minimum, (c) calculated data for choline conformation perpendicular to bilayer surface at lowest *R*-factor minimum.

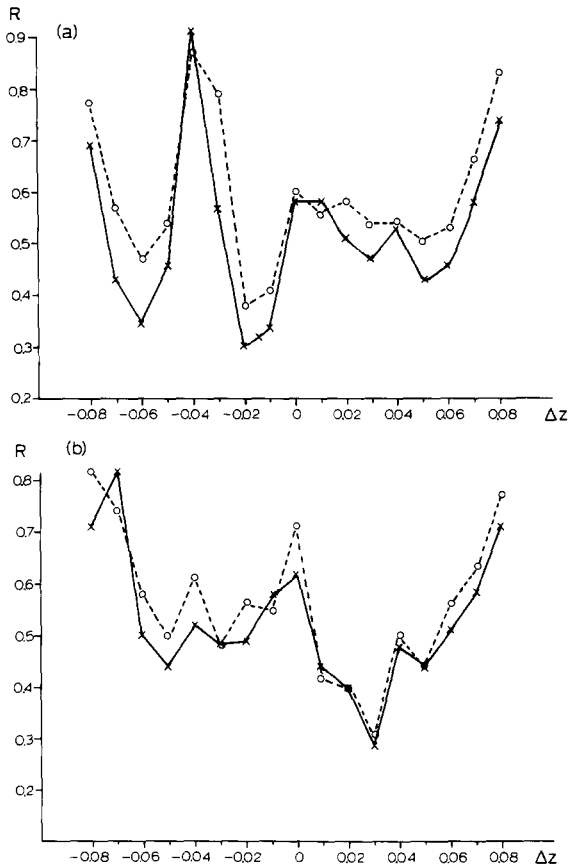

Fig. 6. Translational structure searches for DHPEM form 1. Two different *N*-methyl group positions are included here for each conformer model and are shown to cause slight differences in the plots. In each analysis, the outermost alkyl chain carbon in Fig. 3 was initially placed at $z = 0.5$ and the molecule was then shifted along c and structure factors calculated in space group $P2_1$ (equivalent to $P\bar{1}$ for the 00*l* row) to be compared to observed structure factors: (a) *N*-methylethanolamine parallel to bilayer surface (these *R*-value plots resemble the solid line in Fig. 4), (b) *N*-methylethanolamine perpendicular to bilayer surface (these resemble the *R*-value plot in the dashed line of Fig. 4).

was considered, as suggested by earlier studies of lecithin multilayers [10,12]. A re-analysis of the DHPC structure is shown in Fig. 4 considering both conformations. Because of a corrected methyl carbon position in this analysis, the distinction between two residual minima is now more clear – i.e., for the form with headgroup parallel to the polar surface, the fit of calculated structure factors with observed data is somewhat better than previously reported (Table I). Comparison of Patterson functions calculated from structure factor data for respective headgroup conformers at lowest residual minima (Fig. 5) shows that only one model produces a Patterson map resembling that calculated with observed data. Although the fit of computed and observed structure factor data is improved in this analysis (Table I), the conclusions of the earlier determination [32] are not changed.

Although the Patterson function for form 1 of DHPEM (Fig. 2) is similar to that from DHPC (Fig. 5), it was not assumed a priori that the polar group conformation should be the same for both compounds. Structural models based on the two conformers in Fig. 3 were translated past a unit cell origin to obtain structure factor data for comparison to observed data as before [20,32]. As shown in Fig. 6, there is some sensitivity of the residual minimum values to the placement of the single methyl group on the amino nitrogen (only the three depicted sites occupied in the phos-

TABLE I

OBSERVED AND CALCULATED STRUCTURE FACTOR MAGNITUDES FOR LAMELLAR PHOSPHOLIPIDS (ABSOLUTE VALUES)

DHPC			DHPEM, form 1			DHPEM, form 2		
l	F_c	$\lvert F_0 \rvert$	l	F_c	$\lvert F_0 \rvert$	l	F_c	$\lvert F_0 \rvert$
1	0.34	0.30	1	0.35	0.22	1	−0.25	0.20
2	−0.08	0.07	2	−0.11	0.09	2	0.38	0.36
3	0.12	0.22	3	0.16	0.24	3	0.34	0.41
4	−0.19	0.15	4	−0.17	0.18	4	0.16	0.23
5	−0.09	0.12	5	0.06	0.18	5	0.27	0.20
6	−0.20	0.16	6	−0.18	0.15	6	0.25	0.25
7	−0.14	0.11	7	−0.14	0.11	7	0.21	0.19
8	−0.11	0.14	8	−0.10	0.15	8	0.13	0.15
10	−0.13	0.20	9	−0.14	0.14		$R = 0.17$	
11	−0.19	0.12	10	−0.13	0.20			
12	−0.14	0.14	11	−0.18	0.14			
	$R = 0.26$		12	−0.23	0.23			
			13	−0.22	0.14			
				$R = 0.30$				

phatidylcholine structure were allowed in this analysis) although the positions of the deepest minima are not changed. On the basis of crystallographic residuals, it is not possible to distinguish between the two conformational possibilities for *N*-methylethanolamine in this case [23]. Comparison of calculated Patterson functions from data taken at respective residual minima to the observed Patterson function (Fig. 2b) again shows a superficial resemblance of the two. However, the Patterson function for the headgroup conformation parallel to the bilayer surface best matches the peak positions in the autocorrelation function calculated with observed intensities (Fig. 2c). A comparison of calculated and observed structure factors for this conformer is tabulated in Table I.

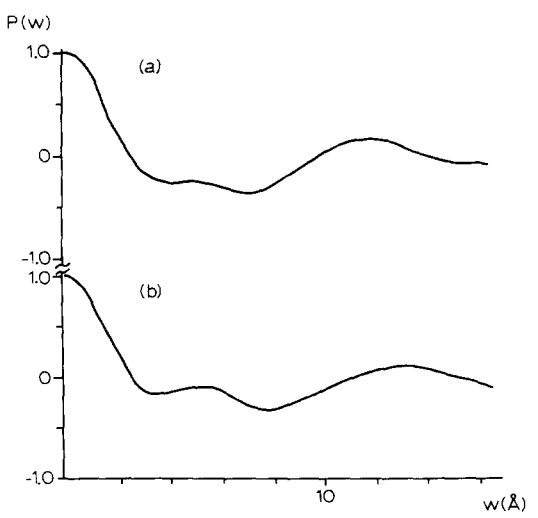

Fig. 7. Patterson function for DHPEM, form 2 (interdigitated bilayer): (a) observed electron diffraction intensities, (b) calculated data at *R*-factor minimum.

Form 2

The Patterson function calculated from observed intensity data from form 2 of DHPEM (Fig. 7) is less easy to interpret than the one in Fig. 2a. Since electron diffraction data from solution-grown crystals indicate that this form also contains untilted molecules, it is clear that only an interdigitated bilayer would explain the small lamellar spacing. For the translational structural analysis, a molecular model based on the same conformation found for DHPC [32] with *N*-methylethanolamine parallel to the bilayer surface was used for generation of calculated structure factors. The map of residual minima vs. molecular shift (Fig. 8) reveals a possible structure solution corresponding to $R = 0.17$, for which the computed Patterson function corresponds well to the observed function (Fig. 8). Observed and calculated structure factors are listed in Table I.

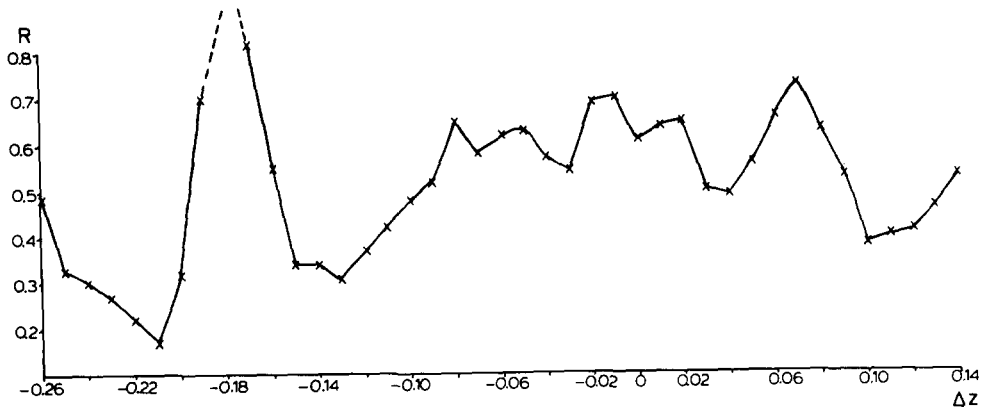

Fig. 8. Translational search of structure solution for DHPEM, form 2. Only a *N*-methylethanolamine headgroup conformation parallel to the bilayer surface is considered. In this search the outermost alkyl chain carbon atom was initially placed at $z = 1.0$ and the molecule was translated by the unit cell origin in $P2_1$ for calculation of $00l$ structure factors.

Lattice images

It is not clear at first how accurately a Fourier-peak-filtered electron micrograph of a phospholipid lamellar packing represents the textural features of the original image, particularly if that image contains lattice imperfections. If the region of the image selected for averaging is nearly perfect (Fig. 9a–c), then the peak filtration should be a fairly close mapping of the original structure. On the other hand, when the image area contains curvilinear distortions (Fig. 9d), leading to arcing of the Fourier transform (Fig. 9e), then the appearance of the reconstruction can vary depending on the hole size in the mask used to screen out the diffuse scattering (Fig. 9f–i). Although none of the reconstructions are exact one-to-one mappings of the defect structures, there is an optimal mask hole size where the phase variation within the arced diffraction peak dominates over any surrounding phase noise which can distort the image. This problem is particularly important for experimental images where the structural details are not readily visible to the naked eye. Experimental electron microscope images have been recorded for both polymorphic forms of DHPEM and their reconstructions often indicates the presence of lattice termination defects and curvilinear distortions (Fig. 10), again justifying the correction to electron diffraction intensities described above, and in previous communications [20,21,32].

It is next of interest to assess how useful such lattice images are for the extraction of low angle phase information. As a test of this, three good lattice images of epitaxially crystallized DHPE [20] which were found to diffract to three orders on an optical bench (diffraction resolution of 18 Å) were reconstructed by Fourier-peak-filtration. At the image magnification used, however, only low diffraction orders were included in the field of the computed transform. First the retrieved phases were corrected for the origin shift r_0 indicated above. The relative phase of the second diffraction peak was then determined after the first-order phase was assigned the values $\phi_{10} = \pi$, (which is the Babinet phase value [33] of the negative image read by the densitometer), corresponding to a crystallographic phase $\psi_{10} = 0$ found in the crystal structure analysis [20]. A second Babinet phase value $\phi_{20} = 0$ is found in these analyses within an error of less than 16° and corresponds to a crystallographic phase $\psi_{20} = \pi$, matching the original crystal structure. Since the phase ψ_{10} is origin-dependent in plane group p2 [26] its value will change from 0 to π depending on whether the origin is chosen at $z = 0$ or $1/2$. The phase ψ_{20}, however, is invariant and should remain the same for either origin definition, an observation which is confirmed by the experimental data.

One good electron image of form 1 of DHPEM gave an optical diffractogram containing two orders of the lamellar repeat. If ϕ_{10} is chosen to be $0, \pi$, then the Babinet value of the p2 invariant phase $\phi_{20} = 0$ corresponding to a crystallographic phase $\psi_{20} = \pi$. Unfortunately both possible struct-

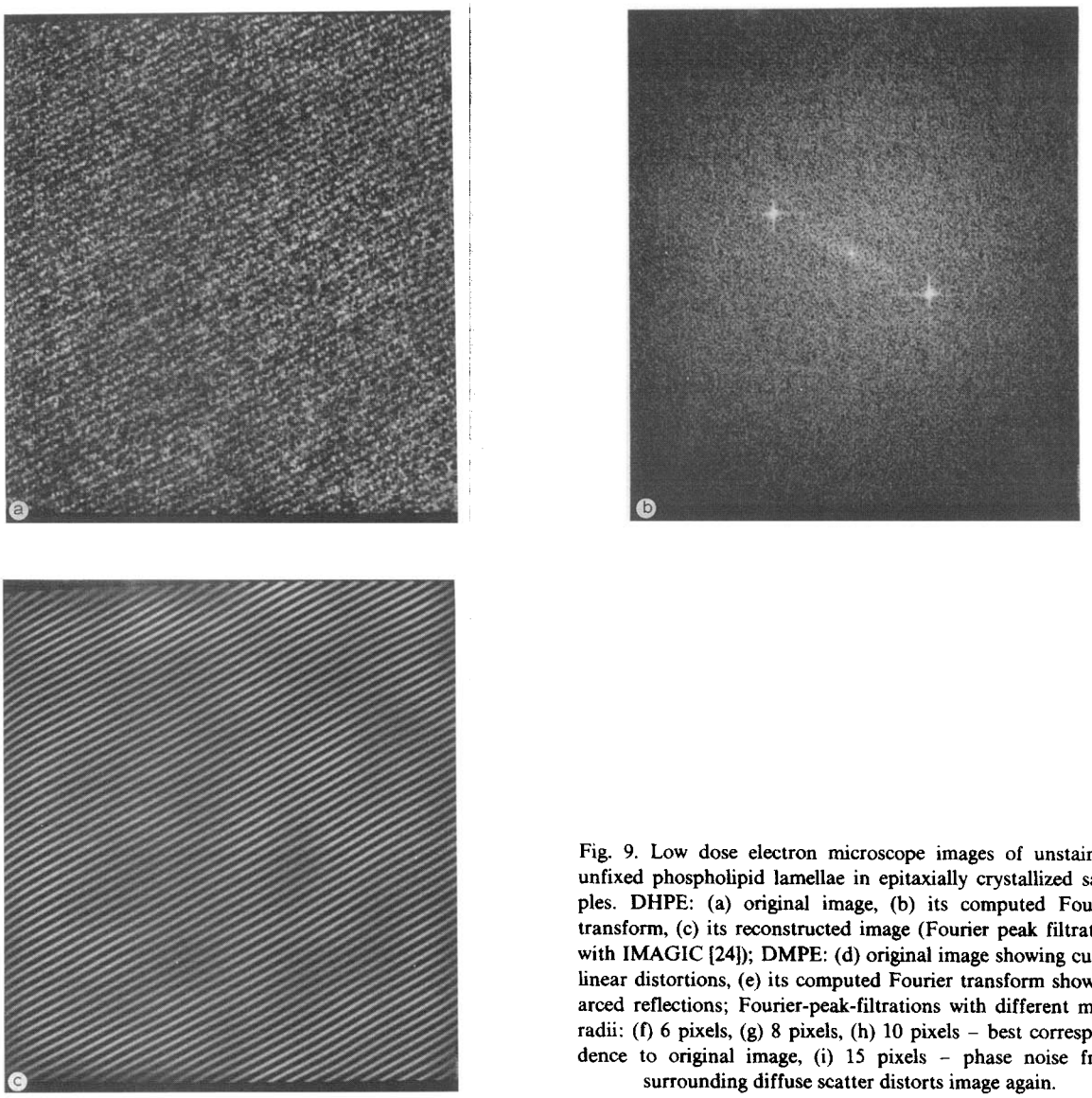

Fig. 9. Low dose electron microscope images of unstained, unfixed phospholipid lamellae in epitaxially crystallized samples. DHPE: (a) original image, (b) its computed Fourier transform, (c) its reconstructed image (Fourier peak filtration with IMAGIC [24]); DMPE: (d) original image showing curvilinear distortions, (e) its computed Fourier transform showing arced reflections; Fourier-peak-filtrations with different mask radii: (f) 6 pixels, (g) 8 pixels, (h) 10 pixels – best correspondence to original image, (i) 15 pixels – phase noise from surrounding diffuse scatter distorts image again.

ural models for this form 1 lamellar packing (Table I) would fit this phase assignment.

Discussion

Using the criterion of matched Patterson functions to determine the correct structure for DHPEM, form 1, it is seen that an untilted bilayer structure with *N*-methylethanolamine oriented parallel to the bilayer surface forms a consistent structural series from DHPE to DHPC. The respective projected phosphorus distances from the unit cell origin (viz.: DHPE, 2.23 Å; DHPEM, 3.19 Å; DHPC, 3.88 Å) parallel the increase of lamellar spacing, indicating that the initial methylation of ethanolamine is reponsible in itself for the lamellar spacing increase, i.e. due to the increased size of the headgroup. All three crystal structures investigated so far involve untilted molecules and contain alkyl chains packing in the same methylene subcell, thus providing a useful way to settle this issue without the added complication of chain

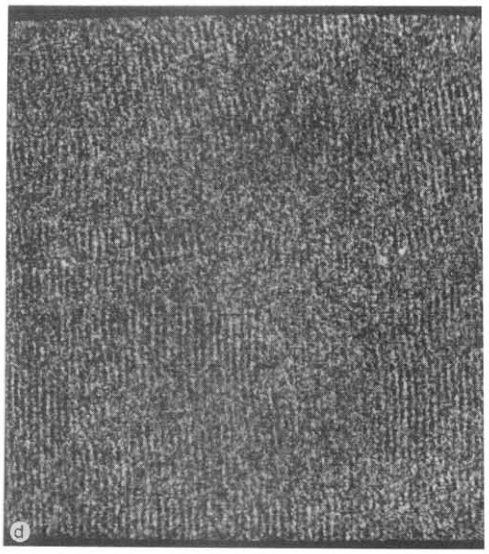
d

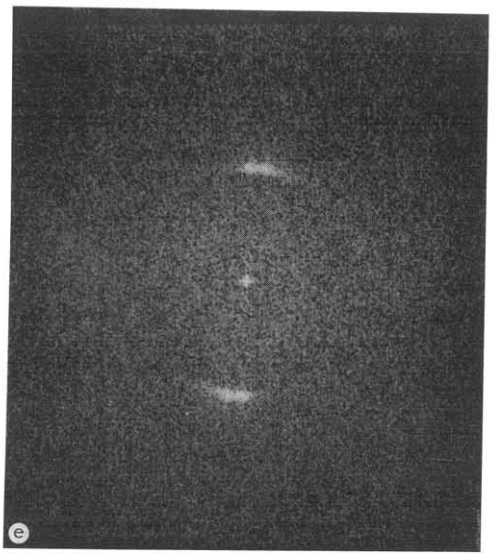
e

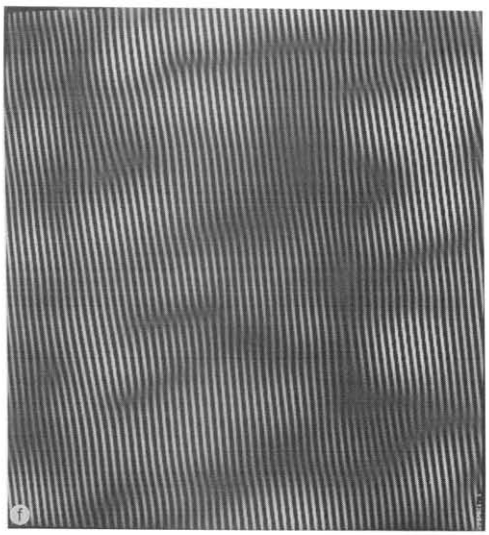
f

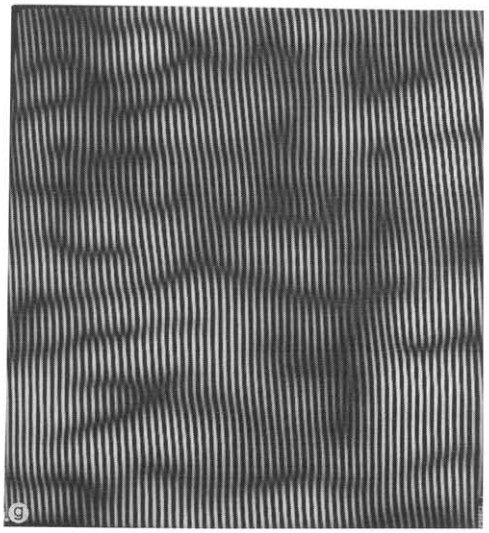
g

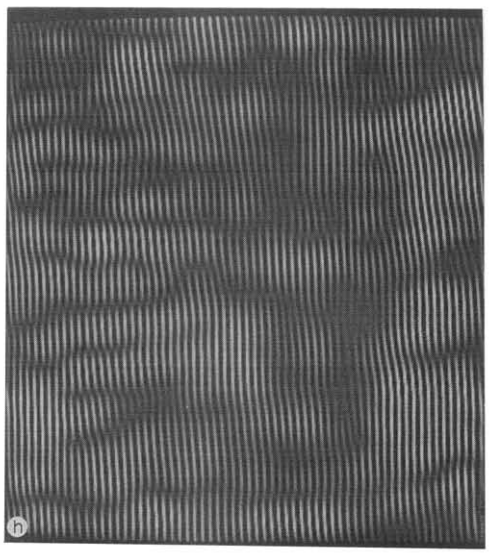
h

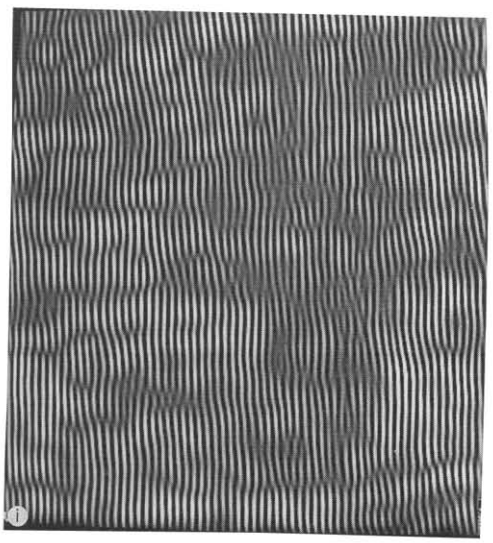
i

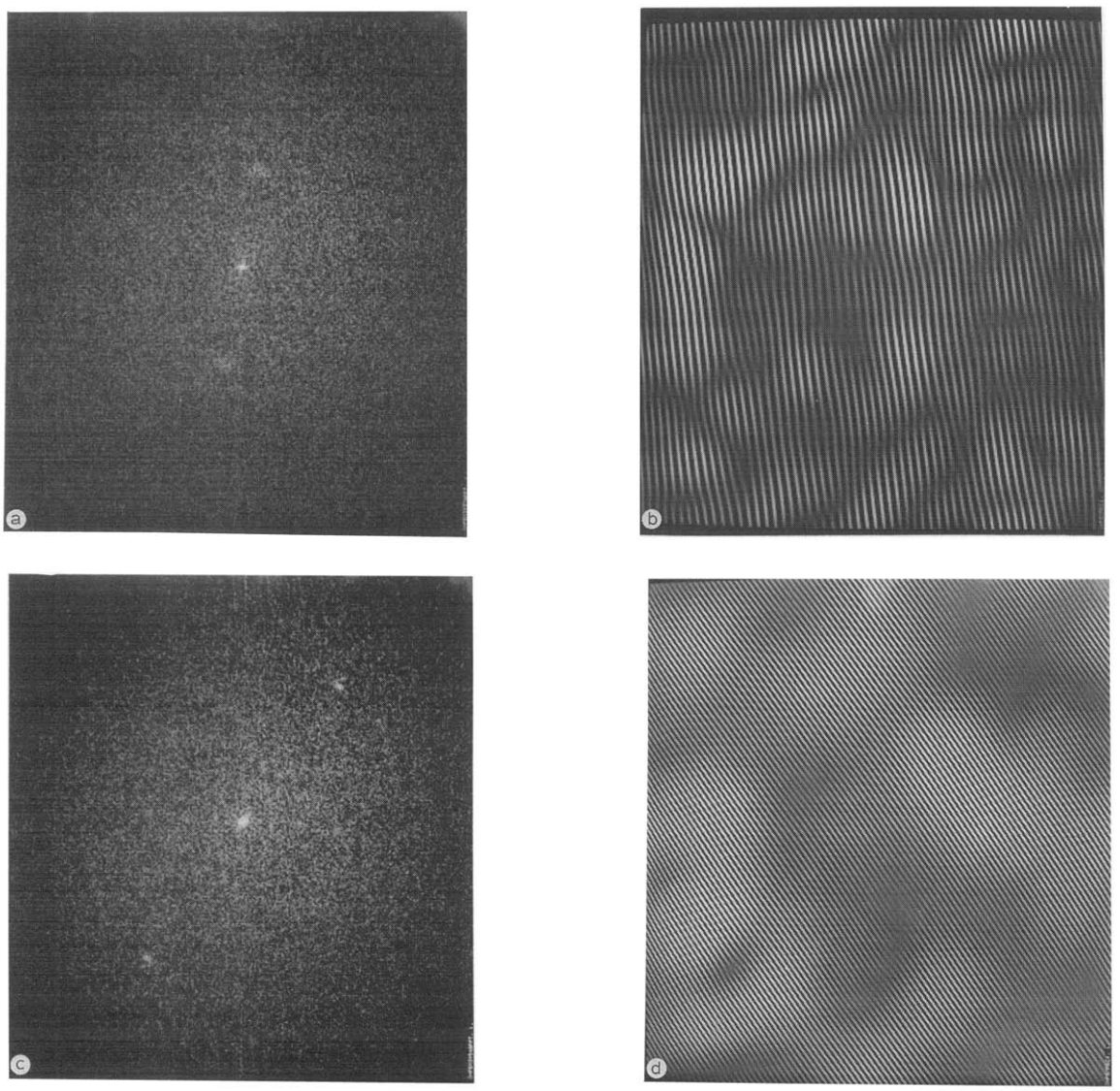

Fig. 10. Reconstructed images of DHPEM; form 1: (a) computed Fourier transform, (b) Fourier-peak-filtered reconstruction showing presence of lattice distortions; form 2: (c) computed Fourier transform, (d) Fourier-peak-filtered reconstruction.

tilt proposed for the intermediate *N*-methyl derivatives [13] and found for phosphatidylcholine [34] in the hydrated state.

The existence of the interdigitated form 2 bilayer is somewhat surprising since this presumably is a minimally solvated structure. This minimal solvation is established by comparing the d_{001} = 33.4 Å to the 30 Å lipid layer distance (but not bilayer repeat) seen in interdigitated DPPC [35] and DHPC [36]. Although the chains are untilted in DHPEM form 2, the structural model found above is consistent with the crystal structures of two lysophosphatidylcholines [37,38] for which the projected phosphorus to origin distance of 1.82 to 1.84 Å can be compared to the 1.52 Å found in this analysis. The presence of an untilted crystalline chain packing is also consistent with solvated interdigitated forms of DPPG [39], DPPC [40], and DHPC [42].

What is unclear is how the headgroup surface

area is compensated by the chain surface areas, i.e. how many chains are present for each polar group? For a typical $0_{\perp}$ methylene packing, the chain cross sectional area is $\Sigma = 18.6$ Å^2 [28]; thus four chains cannot be accommodated per headgroup without $S = 74.4$ Å^2. It is apparent that the large polar group surface areas in this range cannot be achieved without solvation. The rather large cross sectional area found for a lysolecithin monohydrate [37], $S = 52.1$ Å^2 would almost accommodate three untilted chains, i.e. $S/\Sigma = 2.8$. This most likely interdigitated form found for minimally hydrated structures also would stoichiometrically resemble those found for asymmetric diacyl lipids [40,41]. Similar interdigitated forms are found in solid solutions of DMPE with DHPE [42], and are distinguished from those formed by melting anhydrous crystals, which may involve an interdigitation of headgroups instead, similar to the crystal structure of the phosphatidyl-*N*,*N*-dimethylethanolamine [6].

The foregoing represents the first quantitative electron diffraction structural analysis of hitherto uncharacterized phospholipid type and demonstrates the utility of diffraction data from single microcrystals for this purpose since such samples are more easily prepared than those needed for single crystal X-ray experiments. Foregoing analyses on lipids related to known structures have established the consistency of electron diffraction determinations with structures based on other well established diffraction techniques. Although the crystal perfection of epitaxially oriented specimens is somewhere between oriented multilayers and single crystals, the facility of this technique for investigating the nature of polydisperse specimens in particular will be the subject of future quantitative analyses.

Acknowledgement

The author is grateful to the Manufacturers and Traders Trust Company for a grant to fund this research.

References

1 Mulukutla, S. and Shipley, G.G. (1984) Biochemistry 23, 2514–2519.
2 Hitchcock, P.B., Mason, R. and Shipley, G.G. (1977) Proc. Natl. Acad. Sci. USA 71, 3036–3040.
3 Elder, M., Hitchcock, P., Mason, R. and Shipley, G.G. (1977) Proc. Roy. Soc. London A354, 157–170.
4 Pearson, R.H. and Pascher, I. (1979) Nature 281, 499–501.
5 Hauser, H., Pascher, I., Pearson, R.H. and Sundell, S. (1981) Biochim. Biophys. Acta 650, 21–51.
6 Pascher, I. and Sundell, S. (1986) Biochim. Biophys. Acta 855, 68–78.
7 Hitchcock, P.B., Mason, R. and Shipley, G.G. (1975) J. Mol. Biol. 94, 297–299.
8 Suwalsky, M. and Duk, L. (1984) Makromol. Chem. 188, 599–606.
9 Torbet, J. and Wilkins, M.H.F. (1976) J. Theor. Biol. 62, 447–458.
10 Büldt, G., Gally, U., Seelig, J. and Zaccai, G. (1979) J. Mol. Biol. 134, 673–691.
11 Büldt, G. and Seelig, J. (1980) Biochemistry 19, 6170–6175.
12 Worcester, D.L. and Franke, N.P. (1976) J. Mol. Biol. 100, 359–378.
13 Casal, H.L. and Mantsch, H.H. (1983) Biochim. Biophys. Acta 735, 387–396.
14 Wittmann, J.C. and Manley, R.St.J. (1978) J. Polym. Sci. - Polym. Phys. Ed. 16, 1891–1895.
15 Dorset, D.L., Pangborn, W.A. and Hancock, A.J. (1983) J. Biochem. Biophys. Methods 8, 29–40.
16 Jensen, L.H. (1970) J. Polym. Sci. C29, 47–63.
17 Fryer, J.R. (1981) Inst. Phys. Conf. Ser. 61, 19–22.
18 Dorset, D.L. (1985) J. Electron Microsc. Techn. 2, 89–128.
19 Fryer, J.R. and Dorset, D.L. (1987) J. Microsc. (Oxford) 145, 61–68.
20 Dorset, D.L., Massalski, A.K. and Fryer, J.R. (1987) Z. Naturforsch. Teil A, 42a, 381–391.
21 Dorset, D.L. (1987) J. Electron Microsc. Techn. 7, 35–46.
22 Doyle, P.A. and Turner, P.S. (1968) Acta Cryst. A24, 390–397.
23 Hamilton, W.C. (1964) Statistics in Physical Science, pp. 157–160, Ronald, New York.
24 Heel, M.V. and Keegstra, W. (1981) Ultramicroscopy 7, 113–130.
25 Erickson, H.P. (1973) Adv. Optical Electron Microsc. 5, 163–199.
26 Hauptman, H.A. (1972) Crystal Determination. The Role of the Cosine Seminvariants, Plenum Press, New York.
27 Gaskill, J.D. (1978) Linear Systems, Fourier Transforms and Optics, Wiley, New York.
28 Abrahamsson, S., Dahlen, B., Löfgren, H. and Pascher, I. (1978) Progr. Chem. Fats Other Lipids 16, 125–143.
29 Dorset, D.L. (1983) Ultramicroscopy 12, 19–28.
30 Dorset, D.L. (1976) Biochim. Biophys. Acta 424, 396–403.
31 Khare, R.S. and Worthington, C.R. (1978) Biochim. Biophys. Acta 514, 239–254.
32 Dorset, D.L. (1987) Biochim. Biophys. Acta 898, 121–128.
33 Lipson, S.G. and Lipson, H. (1969) Optical Physics, pp. 198–200, Cambridge University Press, London.
34 Zaccai, G., Büldt, G., Seelig, H. and Seelig, J. (1979) J. Mol. Biol. 134, 693–706.
35 McIntosh, T.J., McDaniel, R.V. and Simon, S.A. (1983) Biochim. Biophys. Acta 731, 109–114.

36 Ruocco, M.J., Siminovitch, D.J. and Griffin,R.G. (1985) Biochemistry 24, 2406–2411.
37 Hauser, H., Pascher, I. and Sundell, S. (1980) J. Mol. Biol. 137, 249–264.
38 Pascher, I., Sundell, S., Eibl, H. and Harlos, K. (1986) Chem. Phys. Lipids 39, 53–64.
39 Ranck, J.L., Keira, T. and Luzzati, V. (1977) Biochim. Biophys. Acta 488, 432–441.
40 Hui, S.W., Mason, J.T. and Huang, C. (1984) Biochemistry 23, 5570–5577.
41 McIntosh, T.J., Simon, S.A., Ellington, J.C., Jr. and Porter, N.A. (1984) Biochemistry 23, 4038–4044.
42 Dorset, D.L. and Massalski, A.K. (1987) Biochim. Biophys. Acta 903, 319–332.
43 Green, J.P., Phillips, M.C. and Shipley, G.G. (1973) Biochim. Biophys. Acta 330, 243–253.